Oxid Met (2014) 82:195–208
DOI 10.1007/s11085-014-9487-2

ORIGINAL PAPER

Characterization of Alumina Scales Grown on a 2nd Generation Single Crystal Ni Superalloy During Isothermal Oxidation at 1050, 1100 and 1150 °C

R. Swadźba · L. Swadźba · J. Wiedermann · M. Hetmańczyk · B. Witala

Received: 10 February 2014 / Revised: 10 May 2014 / Published online: 28 August 2014

Abstract This paper concerns microstructural characterization of alumina scales formed on a 2nd generation single crystal Ni superalloy during isothermal oxidation in dry oxygen at 1050, 1100 and 1150 °C for 100 h. Samples for high resolution characterization of Al_2O_3 scales were prepared using a focused ion beam (FIB) method. High resolution TEM and S/TEM techniques were used for a detailed characterization and a direct comparison of the phase composition and chemistry of the oxide scales formed during high temperature oxidation. The growth of transient θ-Al_2O_3 and its transformation to α-alumina is addressed for each oxidation temperature along with the differences in the diffusion of reactive elements, such as Hf, Zr and Y, through grain boundaries of the α phase. The θ to α transformation front was proven to move from the metal-scale to the scale-gas interface. The results presented in this paper indicate that after 100 h of oxidation at 1050 and 1100 °C there are still some θ-alumina grains remaining and even in the regions where the transformation to α was finished the surface retained the whisker-like morphology.

Keywords Alumina · Oxidation · Reactive Elements · Superalloys

Introduction

High temperature resistant materials applied on jet engine blades and vanes rely on their ability to form an adherent and stable oxide scale (thermally grown oxide), mostly Al_2O_3, during high temperature exposure at around 1000–1200 °C [1, 2].

R. Swadźba (✉) · J. Wiedermann
Institute for Ferrous Metallurgy, Gliwice, Poland
e-mail: rswadzba@gmail.com

L. Swadźba · M. Hetmańczyk · B. Witala
Silesian University of Technology, Katowice, Poland

Depending on the temperature, time and substrate composition various polymorphs of alumina can form varying in the structure and growth rate. The most desirable polymorph is the hexagonal α-Al_2O_3 which is characterized by low growth rate and long-term stability at high temperatures. However, prior to the formation of α-alumina various other fast growing transition (metastable) polymorphs can be observed. These include the γ and θ-alumina exhibiting whisker or needle-like morphology which can transform to α-Al_2O_3 with oxidation time [3–7]. While the metastable aluminas grow mostly by outward diffusion of Al^{3+} cations the growth of α-alumina is governed by an inward O^{2-} diffusion, with minor outward Al^{3+} contribution [8–10].

As a result of outward Al^{3+} cationic diffusion and vacancy coalescence during the initial stages of oxidation interfacial voids can form compromising the adhesion of the protective scale and leading to its premature spallation [6, 11–13]. In addition, free surfaces of such voids can serve as segregation sites for indigenous sulfur also weakening the adhesion of oxide scale and promoting void formation [14, 15]. One solution for improving the scale adherence and thus high temperature resistance of superalloys is desulfurization and/or reactive elements (RE) addition that have been proven to provide significant improvements [16, 17].

The addition of reactive elements (RE), such as Hf, Zr and Y, in very small amounts (around 30 ppm in case of Y) to high temperature Ni superalloys provides excellent oxide scale adhesion. These elements diffuse outward through grain boundaries of alumina due to oxygen potential gradient (OPG) and provide some exceptional enhancements in terms of oxide structure and adhesion, including reduction of the oxidation rate, affecting the detrimental effect of sulfur segregation and inhibition of outward Al^{3+} diffusion [18, 19]. While the RE effect has been studied for many decades and detection of RE as grain boundary segregation in alumina scales using STEM–EDS has been commonly reported there is still some debate over the mechanisms by which these oxygen-active elements influence alumina scales [20, 21]. For instance, a recent work conducted by Heuer et al. [21] stated that REs affect the oxidation behavior not by "site blocking" at grain boundaries but by reducing Al ionization and vacancy injection into the scale. In addition to Hf, Zr and Y [22–25] other elements are also commonly found on the grain boundaries of growing alumina scales, such as Ti [22, 26], Ta [26] and La [27].

The growth mechanism and chemistry of thermally grown alumina scales is of great importance particularly in the case of Thermal Barrier Coating systems (TBCs) where alumina TGO bonds the yttria stabilized zirconia (YSZ) with the substrate thus its outward growth would lead to decohesion of the top coat and exhibition of the substrate to high temperature [28, 29]. While the oxidation of modified aluminide bond coatings has been studied in detail by now, during the recent years some interest has been devoted to Pd + Pt [23, 30, 31] modified aluminide coatings that provide excellent oxidation resistance and can be considered as bond coatings for TBC systems. Although bare superalloys are rarely applied on components operating at high temperatures it is important to study their behavior under such conditions in order to evaluate the influence of novel coatings further on. The main purpose of this study was to characterize phase transformations and

segregation phenomena that occur in thermally grown alumina scales during oxidation at three different temperatures: 1050, 1100, 1150 °C for 100 h.

Experimental Procedure

The investigation concerned three samples made of 2nd generation single crystal Ni superalloy (cylinder shaped, 5 mm diameter, 5 mm height) that were oxidized in dry O_2 for 100 h at three different temperatures—1050, 1100, 1150 °C. The alloy's composition was [wt%]: Al-6.14, C-0.06, Co-7.3, Cr-7.3, Hf-0.15, Mo-1.5, Re-2.88, Ta-6.5, W-4.91, Zr-0.01, Y-<0.02, S-0.4 ppm, Ni-balance (determined using XRF, ICP and GDMS). The isothermal oxidation tests were conducted using a Mettler Toledo apparatus. After the oxidation tests the surface microstructures of the samples were studied using FEI Inspect F scanning electron microscope (FEG–SEM). In order to study the microstructure of the oxide scales that formed during high temperature oxidation in detail high resolution S/TEM analysis was performed using FEI TITAN 80–300 microscope equipped with X-FEG. The samples for S/TEM investigation were prepared using Focused Ion Beam method where Pt layer was applied to protect the surface of the oxide scales from the ion (Ga^+) thinning process.

Results

Isothermal Oxidation at 1050 °C for 100 h

The SEM–BSE image of the surface microstructure of the oxide scale formed on the investigated nickel based superalloy during isothermal oxidation at 1050 °C for 100 h is presented in Fig. 1a. STEM–HAADF and BF images of the cross-sectional microstructure of the oxide scale along with electron diffraction patterns for θ and α-Al_2O_3 phases are presented in Fig. 1b,c. The interface between the oxide scale and the superalloy is presented in STEM–HAADF and BF images (Fig. 2a,b) along with elemental mapping of Hf, Ta, Y and Zr on the grain boundaries of α-Al_2O_3 grains presented in Fig. 2c–f.

The surface microstructure of the investigated superalloy after 100 h at 1050 °C is characterized by a whisker-like morphology, often attributed to the θ-Al_2O_3 phase. The detailed STEM analysis allowed differentiating the Al_2O_3 polymorphs present in the cross-section of the oxide scale and made it possible to determine the regions of particular phase's presence. It is noteworthy that in the analyzed region the oxide scale is free from nickel oxides (NiO) or spinels ($NiAl_2O_4$), which indicates that the only oxidizing species was Al. However, it is important to highlight the fact that the STEM sample was extracted from a small fraction of the whole surface. The alumina scale consists of distinctive zones with different microstructures and phase constituents. The outer zone (around 1.5 μm thick) consists of θ-alumina (by electron diffraction) whiskers visible as feather like regions in the STEM–BF image (Fig. 1c) that form the undulated surface visible in

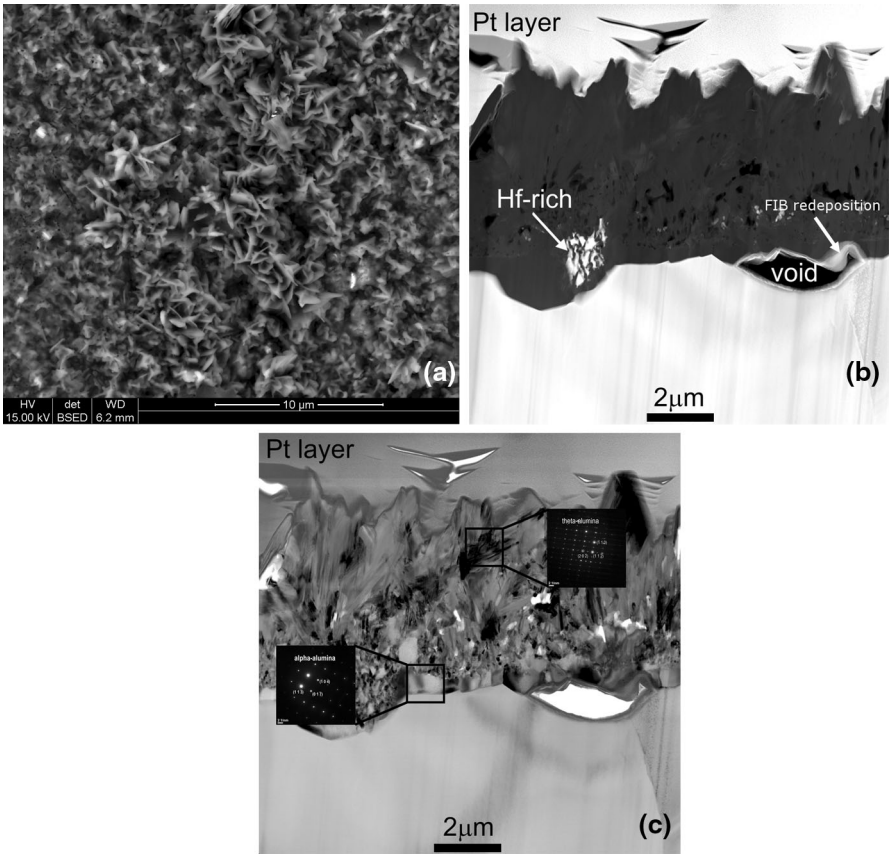

Fig. 1 SEM–BSE image of the surface microstructure (**a**), STEM–HAADF (**b**) and BF (**c**) images of the cross-sectional microstructure of the oxide scale formed on during isothermal oxidation at 1050 °C for 100 h

the Fig. 1a. These transient grains grew by outward cationic (Al^{3+}) diffusion and contain around 0.4 at% Cr. They are relatively dense and highly twinned as previously reported by Doychak et al. [4, 5]. The intermittent porosity within this zone denotes the boundary with the middle zone of the oxide scale where the θ grains have partially transformed to the stable α polymorph which leads to volumetric changes. The mixed θ + α middle zone is around 1.2 µm thick and contains Hf-rich particles with varying sizes, from single nanometers up to even 1 µm wide, as marked on the HAADF image in Fig. 1b. Underneath the middle mixed zone there is a very thin (around 250 nm thick) internal zone consisting exclusively of dense columnar α-alumina grains that nucleated at the interface with the substrate alloy and grew by inward anionic diffusion of O^{2-}. The width of each columnar grain is around 200–350 nm and their characteristic feature is that they form distinctive imprints in the substrate (clearly visible in Fig. 1b) with convex and sharp edges on the grain boundaries of α-alumina. Additionally, each grain boundary is doped with Hf and Ta ions as visible in the HAADF image in Fig. 2a

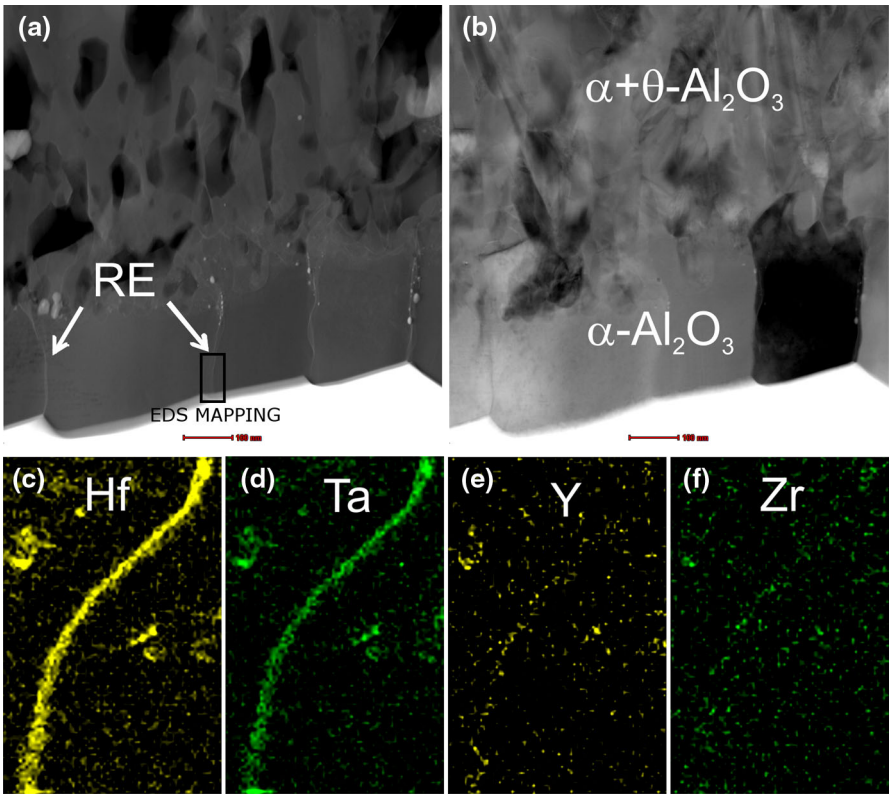

Fig. 2 STEM–HAADF (**a**) and BF (**b**) image of the interface between the oxide scale and the substrate, elemental mapping of Hf (**c**), Ta (**d**), Y (**e**) and Zr (**f**) on the grain boundaries of α-Al_2O_3

(the grain boundaries are visualized as bright regions by the Z-sensitive detector) and proved by the elemental mapping presented in Fig. 2c,d. The EDS signal for both Y and Zr (Fig. 2e,f) is hardly discernible. In addition to the grain boundary segregation of Hf and Ta there are also regions of saturation where nanometric particles nucleated, mostly at the interface with the middle zone of the oxide scale. No trace of ionic segregation of Hf or any other element was found in the regions with transient θ grains. Due to the unbalanced diffusion of cations and anions during the initial stages of oxidation voids can form at the interface with the substrate alloy (Fig. 1b). Such voids can be healed during the inward growth of the columnar α-alumina grains. The void presented in Fig. 1b has not been fully healed by the growing α grains yet. The bright boundaries around it originate from FIB milling process and redeposition of the milled material.

Isothermal Oxidation at 1100 °C for 100 h

The SEM–BSE image of the surface microstructure of the oxide scale formed on the investigated nickel based superalloy during isothermal oxidation at 1100 °C for 100 h is presented in Fig. 3a. STEM–HAADF image (representing the Z contrast)

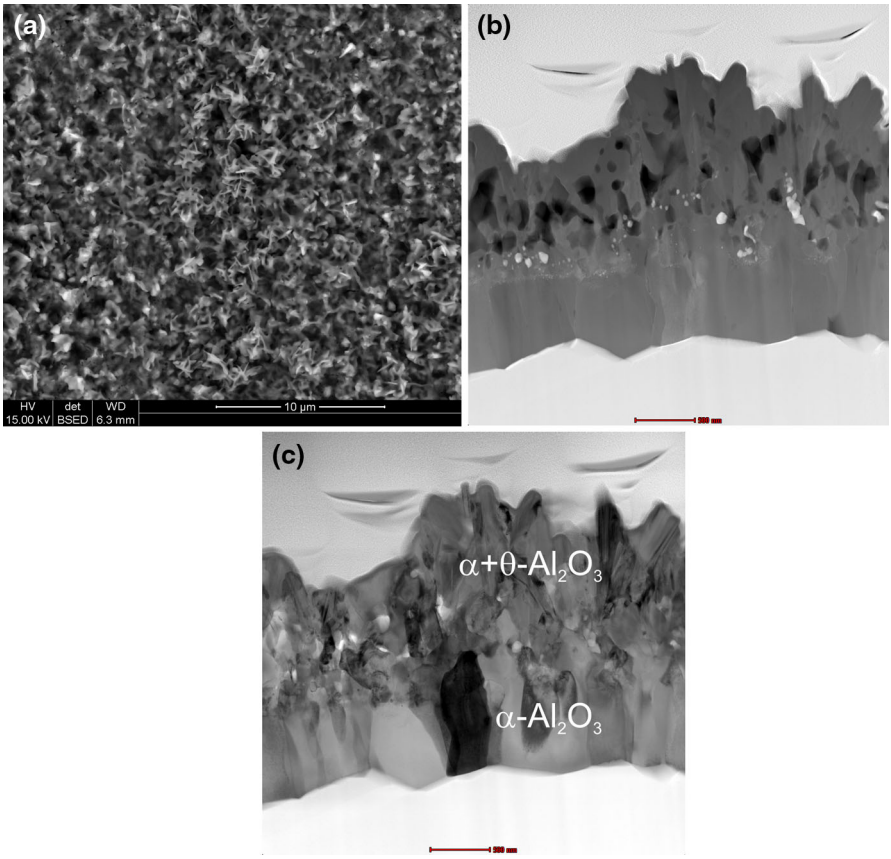

Fig. 3 SEM–BSE image of the surface microstructure (**a**), STEM-HAADF (**b**) and BF (**c**) images of the cross-sectional microstructure of the oxide scale formed during isothermal oxidation at 1100 °C for 100 h

and BF image (representing crystallographic orientation contrast) of the cross-sectional microstructure of the oxide scale are presented in Fig. 3b,c. The outer whisker-like alumina grains are presented in the STEM–BF image in Fig. 4a. The interface between the oxide scale and the superalloy is presented in STEM–HAADF image (Fig. 4b) along with elemental mapping of Ta, Hf, Y and Zr on the grain boundaries of α-Al_2O_3 grains presented in Fig. 4c–f.

The surface microstructure of the oxide scale formed during isothermal oxidation at 1100 °C for 100 h consists of whisker and blade-like grains of alumina, which can indicate the presence of θ and some transformed α-alumina grains. Cross-sectional STEM analysis revealed that the oxide scale is about 2.5 µm thick and consists of two zones. The outer zone (1.5 µm thick) consists mostly of equiaxed and porous α-alumina grains (Fig. 3b,c), however some needle-like and internally twinned θ grains (600–700 nm in length) are still remaining in its upper part forming roughened surface (Fig. 3c and 4a) indicating that the transformation was not finished by the end of the isothermal oxidation test. In addition, the regions of θ phase presence are rougher than those of α. EDS analysis revealed that the outer

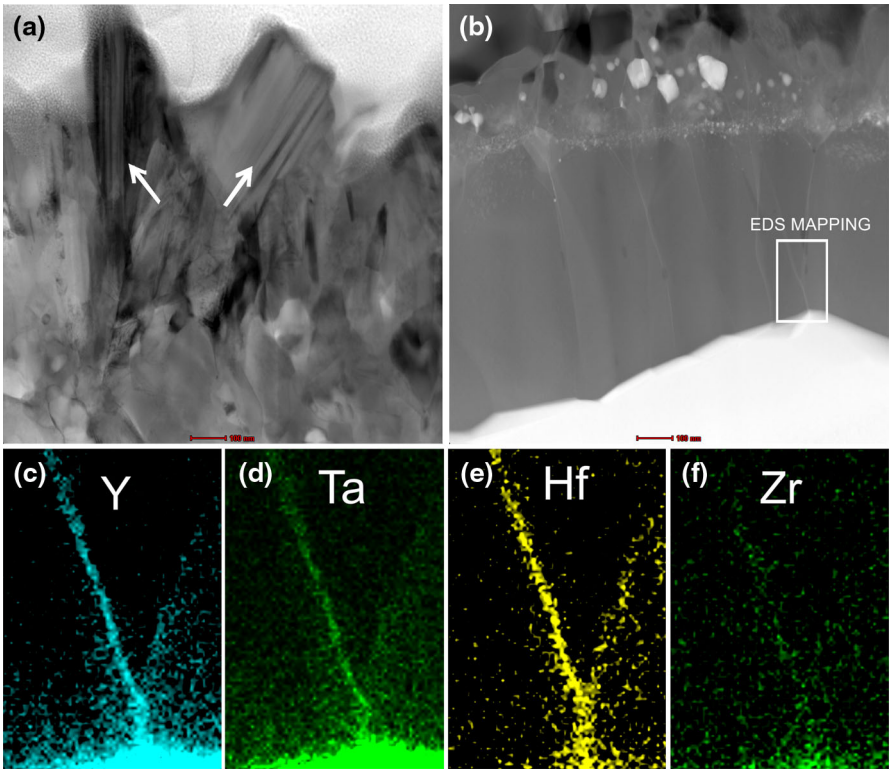

Fig. 4 Microstructure of the oxide scale formed during isothermal oxidation at 1100 °C for 100 h: STEM–BF (**a**) image of the θ-Al_2O_3 twinned grains in the outer zone of the oxide scale and (**b**) inner columnar grains of α-Al_2O_3 along with elemental mapping of Y (**c**), Ta (**d**), Hf (**e**) and Zr (**f**)

zone consisting of the θ and transformed α grains contains around 0.3 at% Cr. The inner zone of the oxide scale ($\sim$1 μm thick) consists of dense columnar α-alumina grains that nucleated between the transformed α grains and the substrate alloy and grew probably by inward O^{2-} diffusion forming distinctive roughened interface beneath them (oxide imprints in the substrate). The average width of the columnar grains is around 300 nm. The grain boundaries of the columnar α-alumina grains appear bright on the STEM–HAADF image (Fig. 4b) indicating the presence of segregants doping the interface. STEM/EDS mapping revealed the presence of not only Hf and Ta but also a strong signal of Y diffusing from the ridge in the imprinted substrate. Similarly to the scale grown at 1050 °C the EDS signal of Zr on that grain boundary was negligible (Fig. 4f).

Isothermal Oxidation at 1150 °C for 100 h

The surface microstructure of the oxide scale formed during oxidation of the investigated superalloy at 1150 °C for 100 h is presented in Fig. 5a. The STEM-HAADF and BF images of the cross-sectional microstructure of the oxide scale are

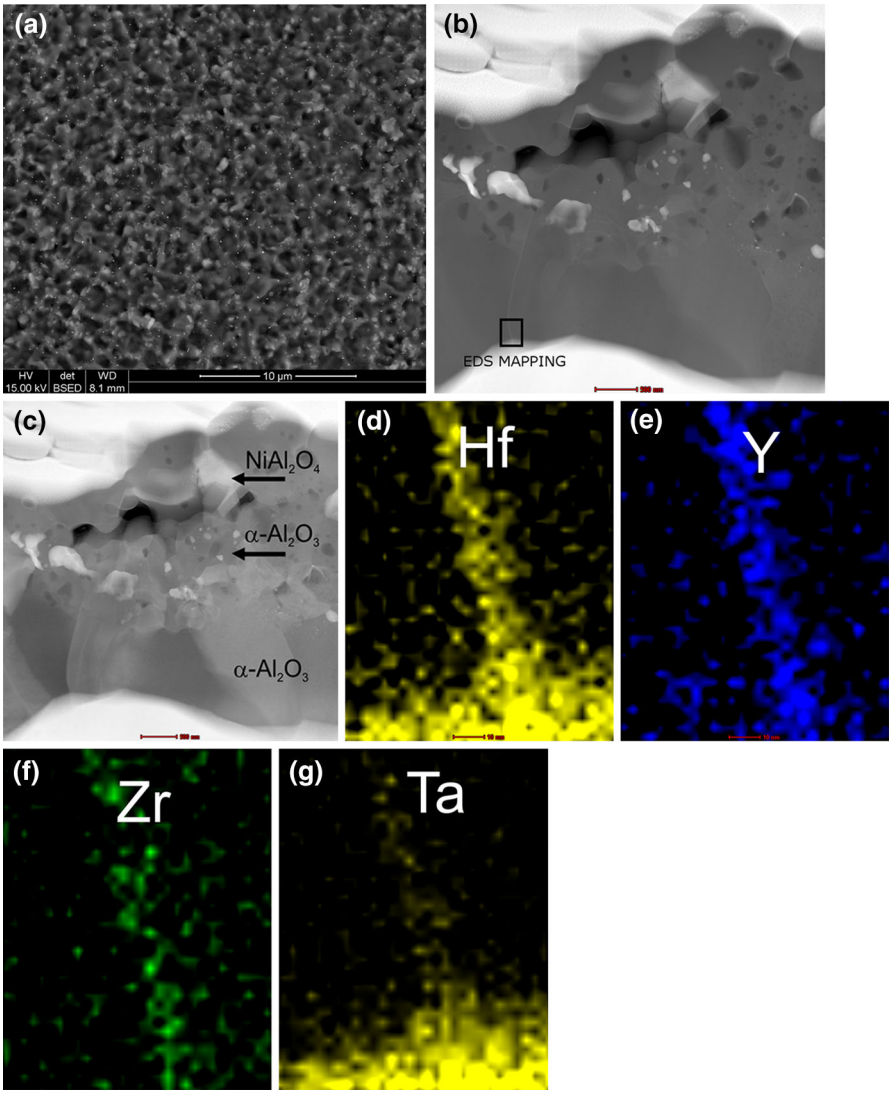

Fig. 5 SEM-BSE image of the surface microstructure (**a**), STEM–HAADF (**b**) and BF (**c**) images of the cross-sectional microstructure of the oxide scale formed during isothermal oxidation at 1150 °C for 100 h, elemental mapping of Hf (**d**), Y (**e**), Zr (**f**) and Ta (**g**) on the grain boudaries of α-Al_2O_3

presented in Fig. 5b,c. The elemental mappings of Hf, Y, Zr and Ta from the grain boundaries of the columnar α-alumina are presented in Fig. 5d–g.

The microstructure of the oxide scale formed during oxidation of the investigated superalloy at 1150 °C for 100 h is characterized by a smoother morphology than that observed during oxidation at 1050 and 1100 °C. The cross-sectional microstructure of the alumina scale is characterized by the presence of two zones and a thickness of around 3.7–4 µm. The outer zone of the oxide scale consists entirely of

α-alumina with distinctive porosity deriving from the θ → α transformation which seems to be complete after 100 h as no remaining grains of θ were found in this study. Additionally, apart from the large pore in the middle of Fig. 5b,c the remaining pores are relatively small (around 200 nm) in comparison to those observed in case of the sample oxidized at 1100 °C. The content of Cr in the outer zone was found to be around 0.4 at%, while no Cr was found in the inner zone. In the STEM–HAADF image (Fig. 5b) it is clearly visible that all the alumina grain boundaries are doped with RE. The elemental mapping performed in the region marked in Fig. 5b revealed the presence of Hf, Ta, Y and Zr diffusing from the substrate alloy. The saturation of these elements at the interface between the outer and inner zone lead to the formation of dispersive oxide precipitates, that include Hf, Zr, Y-rich oxides of various sizes (from single nanometers up to 500 nm). Apart from that there are also Ni-rich oxides, identified as $NiAl_2O_4$ spinel phase, of around 800 nm width. The inner zone of the oxide scale consists of dense and pore-free α-alumina grains with a morphology resembling columnar grains observed at 1050 and 1100 °C.

Discussion

Surface Microstructure of Oxide Scales

The surface microstructures of the oxide scales formed on the investigated nickel superalloy after 100 h at 1050–1100 °C are characterized by a whisker-like morphology, which is commonly attributed to the transition alumina polymorphs. However, this characteristic structure does not necessarily indicate the presence of either γ or θ-Al_2O_3 since, as it was proven by Tolpygo et al. [32], even after the transition to the α-alumina such a structure can be retained for a long time, depending on the oxidation temperature and surface diffusion processes. The results presented in this study confirm this phenomenon as even after 100 h at 1100 °C where seemingly all the θ transformed to α the surface morphology still contains whisker and blade-like grains. However, a direct comparison of the cross-sections of the oxide scales formed during oxidation at 1050, 1100 and 1150 °C for 100 h clearly indicates that the increase in the oxidizing temperature leads to faster surface smoothing. It is directly related to the onset of θ to α transformation which occurs faster at higher temperatures.

S/TEM Analysis of Cross-Sectional Microstructure After 100 h

In the initial stages of oxidation the oxide scale forms as twinned θ-Al_2O_3 that grows by outward diffusion of Al^{3+} cations [3–7] and simultaneous vacancy injection at the metal-scale interface [14] With oxidation time the α-Al_2O_3 grains first form due to nucleation by phase transformation from θ-Al_2O_3 at the metal-scale interface and provide nucleation sites for new α-alumina that then also grows at the metal-scale interface by oxidation reaction involving inward diffusion of O^{2-} by grain boundaries and forms distinctive imprints in the substrate. The nucleation site

of α-Al_2O_3 grains that form either by transformation or oxidation reaction locates at the metal-scale interface is in agreement with results obtained by Smialek et al. [33]. It is noteworthy that even though the predominant diffusing species during the growth of α-alumina is oxygen, experimental work [10] has proven that Al outward diffusion also takes place to a minor extent.

The structure and growth rate of alumina is significantly influenced by the oxidizing temperature as in the case of 1050 °C the majority of alumina is θ with nanometric columnar α grains (250 nm) nucleating by oxidation reaction at the interface with the substrate while at 1150 °C the columnar α grains constitute almost 50 % of the scale thickness (around 1.5 μm) and all θ grains are transformed. In addition, this comparison shows that the θ → α transformation front moves from the metal-scale to the scale-gas interface with simultaneous inward growth of the columnar α-alumina grains that nucleated by oxidation reaction. The microstructure of alumina that formed at 1100 °C is somewhat intermediate since columnar α-alumina grains nucleated and grew to around 1 μm thickness yet in the outer zone some remaining twinned θ grains were still present. The presence of θ proves that the transformation to α was not finished after 100 h of oxidation in case of samples oxidized at 1050 and 1100 °C. The influence of temperature is also expressed by the thickness of oxide layers which formed by phase transformation and oxidation reaction. While in case of the oxide scale formed during oxidation at 1050 °C it is difficult to measure the thickness of the zone where only transformed α grains are present these can be easily distinguished in oxide scales formed at 1100 and 1150 °C. Furthermore, the thickness of the zone with α grains that formed due to phase transformation was found to decrease with oxidizing temperature while the opposite was observed for the columnar α grains which nucleated by oxidation reaction. This confirms that at higher temperatures the θ phase is present for shorter time and undergoes phase transformation to α faster than at lower temperatures thus the oxidation reaction leading to formation of the columnar α grains occurs earlier.

Void Formation

During the growth of thermally grown oxides several types of voids can form [12] that include interfacial voids, intergranular voids and pores that form inside the grains. The observed porosity in the α grains is most probably caused by the transformation from θ and volumetric changes that accompany it [8, 12]. While at 1050 °C the outer zone consists of θ-alumina in case of 1100 and 1150 °C the voids formed during transformation vary in size significantly. As a matter of fact, they are larger in the scale formed at 1100 °C which can indicate that the θ phase grew and remained for a longer period of time leading to the formation of larger voids. At 1050 °C the scale is not fully transformed thus the voids are much smaller.

Although dense, the nucleated columnar α-alumina grains can also contain porosity caused by incorporation of interfacial voids during their inward growth [12, 34]. These voids usually form during transient oxidation period when the oxide scale forms by outward Al^{3+} diffusion. Additionally, they can be the regions for sulfur segregation leading to weakening of the scale adhesion [14, 15, 34]. The studied superalloy contained very low sulfur level (0.4 ppm) and no interfacial

voids were found after oxidation at 1100 and 1150 °C which indicates that even if formed they were most probably healed during the inward growth of alumina when the growth mechanism was dominated by inward oxygen diffusion instead of outward aluminum diffusion. In case of oxidation at 1050 °C a relatively large void (1 μm width) parallel to the interface was observed (Fig. 1a,b). Nucleation of α-alumina grains above the void proves that evaporation and transport of Al across the void takes place [35, 36].

Reactive Element Effect

In order to correctly assess the influence of particular coatings on the behavior of REs it is important to study it first on bare superalloys thus eventual inhibition or enhancement of their diffusion due to the presence of other elements can be evaluated. For instance, our previous study [23] found Zr and Y on the grain boundaries of alumina TGO grown in TBC system (N5 superalloy with Pd–Pt-aluminide bond coating and 7 wt% YSZ top coating) that can lead to argument whether these elements originate from the substrate alloy or the YSZ top coat. The dynamic segregation theory (DST) [16] and the results presented in this work indicate that Zr as well as Y readily diffuses through the grain boundaries of alumina grown on bare superalloy even at very low concentrations.

The behavior of the Reactive Elements (Hf, Y and Zr) differs significantly among the scales formed during oxidation for 100 h at the studied temperatures—1050, 1100 and 1150 °C. The elemental mappings reveal that at the lowest oxidizing temperature (1050 °C) only Hf could be found diffusing through the grain boundaries. With the increase of the oxidizing temperature additional segregants could be found—Y at 1100 °C and both Zr and Y at 1150 °C. Other research works reported Hf diffusing through grain boundaries of oxide scales formed during high temperature oxidation of bare X4 superalloy oxidized at 1100 °C [22] and also on bare N5 superalloy oxidized at 1130 °C [25]. Both Hf and Y were found on grain boundaries of alumina scales formed on Pt-diffused and NiPtAl coated N5 superalloy oxidized at 1150 °C [25, 37] as well as on 1484 coated with MCrAlYHfSi and oxidized at 1100 °C [24]. Zr was reported to segregate at 1100 °C on bare N5 superalloy and at 1200 °C on La_2O_3-dispersed FeCrAl [25]. The results of grain boundary elemental mappings indicate temperature dependence of segregant types. However, contrary to this study other studies of Rene N5 oxidized at 1100 °C for 100 h did not reveal significant [25] or any [39] Y segregation even at its higher content in the alloy (50 ppm). Additionally no Ta was detected in study [25] at 1100 °C while Zr was detected. It is in agreement with the conclusions drawn in these articles that the amount of segregation is not proportional to substrate concentration. Furthermore, since ΔG for Y is higher than that for Zr (−751 vs. −834 kJ/mole cation at 1400 K), which is present at a higher content in the studied alloy yet was not detected in this study at 1050 or 1100 °C, it seems that segregation is not proportional to ΔG either. The differences in segregants detection among the results obtained for alloys of similar compositions indicate that some other phenomena could be responsible for the presence or absence of particular elements on the grain boundaries. One explanation could be

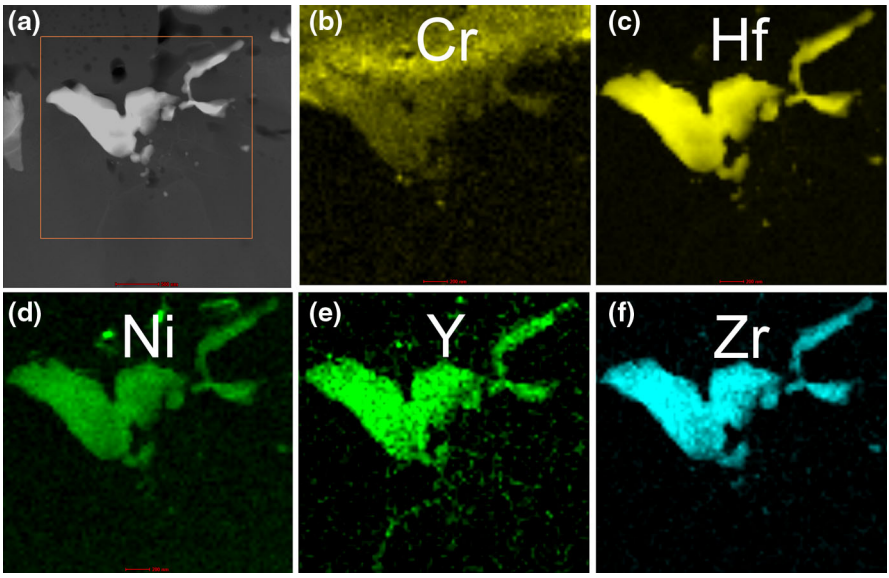

Fig. 6 STEM–HAADF image of the microstructure at the boundary between the outer and inner zone of alumina scale formed at 1150 °C (**a**), elemental distribution of **b** Cr, **c** Hf, **d** Ni, **e** Y, **f** Zr

the fact that, as postulated by Heuer et al. [21], not all grain boundaries are equal and segregation is dependent on the depth of scale [25]. In addition, the zone axis of the single crystal alloy in which the sample is taken could also have effect on the composition of the oxide scale. The latter is a subject of our current research.

It is noteworthy that no segregation was found using EDS in the θ phase region, either on the grain boundaries or twinned areas. Additionally it is supported by lack of any contrast on the STEM–HAADF images (doped regions would appear brighter). What is more, the literature data indicates that the effect of RE additions on the growth of θ-Al2O3 should be minimal and segregation is not expected since RE ions are accommodated more easily in its lattice and the driving force for segregation is removed [38].

The results obtained in this research indicate the following mechanism of RE diffusion through the analyzed alumina scales: the onset of RE diffusion occurs when first α grains nucleate by oxidation reaction at the metal-scale interface while the remaining scale consists of θ and a few transformed α grains. At this point saturation of RE content at the interface between the α and θ + α zones takes place leading to the formation of RE-rich particles. The size of RE-rich particles observed in this study was up to 1 μm in width which is relatively large in respect to the scale thickness. An example of the boundary between the inner (nucleated by oxidation reaction) and outer (nucleated by phase transformation from θ) α-Al_2O_3 zones formed during oxidation at 1150 °C for 100 h which contains RE-rich particles is presented in Fig. 6 along with elemental mapping of Zr, Hf and Y. Additionally, the Cr mapping (Fig. 6b) reveals that the outer zone which initially grew as transient alumina is enriched in this element in contrast to the inner zone that nucleated at the

metal-scale interface. The presence of Cr was noticed for transformed alumina formed at all studied temperatures (1050, 1100, 1150 °C) indicating a higher solubility of Cr in θ in contrast to α. In addition to Hf, Zr and Y grain boundary diffusion of Ta was found at all studied oxidizing temperatures after 100 h. It was also present in the precipitates forming in the oxide scale. Contrary to the mentioned REs Ta does not enhance the durability of the oxide scale [38]. The state of Ta on the grain boundaries of growing alumina scales is considered as ionic although the Al_2O_3 is a more stable oxide than Ta oxides. However, as suggested by Pint et al. [26] since the driving force for diffusion of dopants along the scale grain boundaries is the oxygen potential gradient then it is important which cations are most attracted to oxygen. Thus the free energy of oxide formation per mole cation should be taken under consideration. The calculated ΔG per mole of Ta cation is lower than that per mole of Al cation at 1400 K (−720 vs. −613 kJ/mole cation) and could explain the presence of Ta ions on the grain boundaries.

Summary

The conducted investigation concerned alumina scales grown on 2nd generation single crystal Ni superalloy oxidized at 1050, 1100 and 1150 °C for 100 h. The presented results indicate a significant influence of oxidation temperature on the phase and chemical composition of the alumina scales. With increasing temperature the amount of α in respect to θ-alumina increases as the transformation front moves from the metal-scale interface towards the surface. The transformed α grains are characterized by a porous microstructure due to volumetric changes and are enriched with ~0.4 at% Cr. It was concluded that they serve as nucleation sites for new columnar α grains that grow inwards by O^{2-} diffusion leading to formation of distinctive imprints in the substrate. Even after the θ → α transformation the surface of the oxide scale retained the whisker-like morphology at 1050 and 1100 °C. Ionic segregation of reactive elements was found at grain boundaries of oxide scales formed at all temperatures: Hf at 1050 °C, Hf and Y at 1100 °C, Hf, Y and Zr at 1150 °C. Moreover, the grain boundaries were doped with Ta which is not considered as beneficial.

Acknowledgments The authors would like to thank Dr R. Przeliorz for helpful comments and discussions. Financial support of Structural Funds in the Operational Programme—Innovative Economy (IE OP) financed by the European Regional Development Fund Project No. POIG.0101.02-00-015/08 is gratefully acknowledged.

References

1. S. Bose, *High Temperature Coatings*, Elsevier, 2007.
2. N. Birks, G.H. Meier, F.S. Pettit, *Introduction to the High-temperature Oxidation of Metals*, 2nd edn. Cambridge University Press, 2006.

3. A. G. Evans, D. Clarke and C. Levi, *The Journal of the European Ceramic Society* **28**, 1405 (2008).
4. J. Doychak and M. Ruhle, *Oxidation of Metals* **31**, 431 (1989).
5. J. Doychak, J. L. Smialek and T. E. Mitchell, *Metallurgical and Materials Transactions A* **20**, 499–518 (1989).
6. J.L. Smialek, R. Gibala, In: R.A. Rapp (Ed.), *High Temperature Corrosion* NACE 274–284 (1981).
7. G. Rybicki and J. L. Smialek, *Oxidation of Metals* **31**, 275 (1989).
8. A. H. Heuer, D. B. Hovis, J. L. Smialek and B. Gleeson, *The Journal of the American Ceramic Society* **94**, 146–153 (2011).
9. A.H. Heuer, T. Nakagawa, M.Z. Azar, D.B. Hovis, J.L. Smialek b, B. Gleeson, N.D.M. Hine, H. Guhl, H.-S. Lee, P. Tangney, W.M.C. Foulkes, M.W. Finnis, *Acta Materialia* **61**, 6670–6683 (2013).
10. V. K. Tolpygo and D. R. Clarke, *Materials at High Temperatures* **20**, 261–271 (2003).
11. H. J. Grabke, D. Weimer and H. Viefhaus, *Applied Surface Science* **47**, 243 (1991).
12. B. A. Pint, *Oxidation of Metals* **48**, 303 (1997).
13. R. Swadźba, J. Wiedermann,M.Hetmańczyk, L. Swadźba, B.Witala, G. Moskal, B.Mendala, Ł. Komendera, Materials and Corrosion (2013), http://dx.doi.org/10.1002/maco.201307231.
14. J. A. Haynes, *Scripta Materialia* **44**, 1147 (2001).
15. L. Rivoaland, V. Maurice and P. Marcus, *Oxidation of Metals* **60**, 159 (2003).
16. B. A. Pint, Oxidation of Metals**45**, 1–37 (1996).
17. J. Smialek, *JOM* **52**, 22–25 (2000).
18. D. P. Whittle and J. Stringer, *Philosophical Transactions of the Royal Society of London. Series A* **295**, 309–329 (1980).
19. B. A. Pint, *Oxidation of Metals* **45**, 1–37 (1996).
20. B. A. Pint, I. G. Wright, W. Y. Lee, Y. Zhang, K. Prussner and K. B. Alexander, *Materials Science and Engineering* **A245**, 201–211 (1998).
21. A. H. Heuer, D. B. Hovis, J. L. Smialek and B. Gleeson, *The Journal of the American Ceramic Society* **94**, 146–153 (2011).
22. K. A. Unocic, C. M. Parish and B. A. Pint, *Surface and Coatings Technology* **206** (7), 1522–1528 (2011).
23. R. Swadźba, J. Wiedermann, M. Hetmańczyk, L. Swadźba, B. Mendala, B. Witala and Ł. Komendera, *Surface & Coatings Technology* **237**, 16–22 (2013).
24. K. A. Unocic and B. A. Pint, *Surface & Coatings Technology* **205**, 1178–1182 (2010).
25. B. A. Pint and K. L. More, *The Journal of Materials Science* **44**, 1676–1686 (2009).
26. B. A. Pint and K. B. Alexander, *The Journal of The Electrochemical Society* **145**, 1819–1829 (1998).
27. N. Hiramatsu and F. H. Stott, *Oxidation of Metals* **51**, 479–494 (1999).
28. V. K. Tolpygo and D. R. Clarke, *Surface and Coatings Technology* **200**, 1276–1281 (2005).
29. V. K. Tolpygo and D. R. Clarke, *Materials at High Temperatures* **20**(3), 261–271 (2003).
30. R. Swadźba, M. Hetmańczyk, J. Wiedermann, L. Swadźba, G. Moskal, B. Witala and K. Radwański, *Surface and Coatings Technology* **215**, 16–23 (2013).
31. R. Swadźba, M. Hetmańczyk, M. Sozańska, B. Witala and L. Swadźba, *Surface and Coatings Technology* **206**, 1538–1544 (2011).
32. V. K. Tolpygo and D. R. Clarke, Microstructural study of the theta–alpha transformation in alumina scales formed on nickel aluminides. *Materials at High Temperatures* **17**(1), 59–70 (2000).
33. J. L. Smialek and R. Gibala, *Metallurgical and Materials Transactions A* **14**, 2143–2161 (1983).
34. J. A. Haynes, B. A. Pint, K. L. More, Y. Zhang and I. G. Wright, *Oxidation of Metals* **58**, 513–544 (2002).
35. H. Hindam, D. P. Whittle, *Oxidation of Metals* 245-284 (1982) .
36. J. Angenete and K. Stiller, *Oxidation of Metals* **60**, 83–100 (2003).
37. K. A. Unocic and B. A. Pint, *Surface and Coatings Technology* **215**, 30–38 (2013).
38. B. A. Pint, J. R. Martin and L. W. Hobbs, *Solid State Ionics* **78**, 99–107 (1995).
39. B. A. Pint, K. L. More, I. G. Wright and P. F. Tortorelli, *Materials at High Temperatures* **17**, 165–171 (2000).